Oxo-Bridged Iron Clusters. Synthesis of 1,3-Bis(1,4,7-triaza-1-cyclononyl)-2-hydroxypropane and Its Stabilization of the Fe_4O_6 Core

Jonathan L. Sessler,* John W. Sibert, Anthony K. Burrell, and Vincent Lynch

Department of Chemistry and Biochemistry, University of Texas at Austin, Austin, Texas 78712

John T. Markert* and Chris L. Wooten

Department of Physics, University of Texas at Austin, Austin, Texas 78712

Received April 8, 1993®

The syntheses of the new ligand 1,3-bis(1,4,7-triaza-1-cyclononyl)-2-hydroxypropane, **2**, and the tetranuclear iron(III) complex which it stabilizes are presented. The ligand contains two distinct, macrocyclic binding sites covalently linked via a 2-hydroxypropyl group. The reaction of $2Fe_2$ with triethylamine in either the presence or absence of a carboxylate source results in the formation of a green tetranuclear iron(III) complex, **4**. In addition, the reaction of ligand **2**, $Fe(BF_4)_2$, and sodium benzoate, followed by exposure to oxygen, produces a green solid which is spectroscopically identical to **4**. Complex **4**, $C_{36}H_{86}N_{12}O_{10}P_4F_{24}Fe_4$, forms green crystals in the orthorhombic space group $P2_12_12_1$ (No. 19), with the following unit cell parameters: $a = 15.360(3)$ Å, $b = 16.150(3)$ Å, $c = 25.225(3)$ Å, $V = 6257(2)$ Å^3, and $Z = 4$. The structure of **4** contains a quadruply-charged, tetranuclear iron(III) cation capped by two molecules of **2** which act as ditopic, hepatadentate ligands. The Fe_4O_6 core is composed of a tetrahedron of iron atoms bridged by six oxygen atoms (two oxo, two hydroxo, and two alkoxo groups from ligand **2**). This results in an adamantane-like geometry with the iron atoms occupying the bridgehead positions. The iron atoms are antiferromagnetically coupled ($\mu_{eff} = 1.81\ \mu_B$/Fe at 300 K; 0.26 μ_B at 40 K). Unable to determine precisely the three unique coupling pathways in **4**, we have modeled the magnetic behavior by emphasizing only the dominant oxo-mediated pathway. In this case, there is excellent agreement between theory and experiment with a value for the magnetic exchange coupling constant, J, of $-93(2)$ cm^{-1}.

Introduction

The various roles of iron in biology have been the focus of intense study for many years. In addition to the well-studied iron–heme[1] and iron–sulfur proteins,[2] there is a class of iron-containing proteins which is distinguished from the others by the presence of non-heme, oxo-bridged polynuclear iron cores.[3] The iron–oxo cores in these proteins have proven to be quite versatile biological units. For example, their functions include dioxygen transport (hemerythrin),[4] reduction of ribo- to deoxyribonucleotides (ribonucleotide reductase),[5] acid phosphatase activity (purple acid phosphatase),[6] oxidation of methane to methanol (methane monooxygenase),[7] and iron storage (ferritin and hemosiderin).[8] Of these proteins, the only one that is not a dinuclear iron system is ferritin, which contains a core of up to 4500 iron atoms. In biology, no other examples of oxo-bridged iron oligomers with nuclearities greater than two are currently known.

Within the past decade, attempts to understand both the structure and function of non-heme, iron–oxo proteins through the study of model compounds have led to the discovery of many iron–oxo aggregates with varying nuclearities (Fe_2,[9] Fe_3,[10] Fe_4,[11] Fe_6,[12] Fe_8,[13] Fe_{10},[14] Fe_{11},[15a] Fe_{12},[15b] and other[15c]). These complexes

* Abstract published in *Advance ACS Abstracts*, September 1, 1993.

(1) For a review, see: *The Porphyrins*; Dolphin, D., Ed.; Academic Press: New York, 1978–1979.
(2) For a review, see: *Iron-Sulfur Proteins*; Lovenberg, W., Ed.; Academic Press: New York, 1973–1977.
(3) (a) Vincent, J. B.; Olivier-Lilley, G. L.; Averill, B. A. *Chem. Rev.* **1990**, *90*, 1447–1467. (b) Que, L., Jr.; Scarrow, R. C. In *Metal Clusters in Proteins*; Que, L., Jr., Ed.; ACS Symposium Series 372; American Chemical Society: Washington, DC, 1988, 152–178. (c) Lippard, S. J. *Angew. Chem., Int. Ed. Engl.* **1988**, *27*, 344–361. (d) Lippard, S. J. *Chem. Br.* **1986**, 222–229.
(4) (a) Wilkins, P. C.; Wilkins, R. G. *Coord. Chem. Rev.* **1987**, *79*, 195–214. (b) Klotz, I. M.; Kurtz, D. M., Jr. *Acc. Chem. Res.* **1984**, *17*, 16–22. (c) Wilkins, R. G.; Harrington, P. C. *Adv. Inorg. Biochem.* **1983**, *5*, 51–85. (d) Klotz, I. M.; Klippenstein, G. L.; Hendrickson, W. A. *Science* **1976**, *192*, 335–344.
(5) (a) Norlund, P.; Sjoberg, B.-M.; Eklund, H. *Nature (London)* **1990**, *345*, 593–598. (b) Sjoberg, B.-M.; Graslund, A. *Adv. Inorg. Biochem.* **1983**, *5*, 87–110.
(6) (a) Averill, B. A.; Davis, J. C.; Burman, S.; Zirino, T.; Sanders-Loehr, J.; Loehr, T. M.; Sage, J. T.; Debrunner, P. G. *J. Am. Chem. Soc.* **1987**, *109*, 3760–3767 and references cited therein. (b) Antanaitis, B. C.; Aisen, P. *Adv. Inorg. Biochem.* **1983**, *5*, 111–136.
(7) (a) Dalton, H. *Adv. Appl. Microbiol.* **1980**, *26*, 71–87. (b) Woodland, M. P.; Dalton, H. *J. Biol. Chem.* **1984**, *259*, 53–59. (c) Woodland, M. P.; Patil, P. S.; Cammack, R.; Dalton, H. *Biochem. Biophys. Acta* **1986**, *873*, 237–242.
(8) (a) Theil, E. C. *Annu. Rev. Biochem.* **1987**, *456*, 289–315. (b) Theil, E. C. *Adv. Inorg. Biochem.* **1983**, *5*, 1–38.
(9) Review: Kurtz, D. M., Jr. *Chem. Rev.* **1990**, *90*, 585–606.
(10) (a) A review of trinuclear iron complexes containing the "basic iron acetate" structure: Cannon, R. D.; White, R. P. *Prog. Inorg. Chem.* **1988**, *36*, 195–298. (b) Gorun, S. M.; Lippard, S. J. *J. Am. Chem. Soc.* **1985**, *107*, 4568–4570. (c) Poganiuch, P.; Liu, S.; Papaefthymiou, G. C.; Lippard, S. J. *J. Am. Chem. Soc.* **1991**, *113*, 4645–4651. (d) Gorun, S. M.; Papaefthymiou, G. C.; Frankel, R. B.; Lippard, S. J. *J. Am. Chem. Soc.* **1987**, *109*, 4244–4255. (e) Vankai, V. A.; Newton, M. G.; Kurtz, D. M., Jr. *Inorg. Chem.* **1992**, *31*, 341–343.
(11) (a) McCusker, J. K.; Vincent, J. B.; Schmitt, E. A.; Mino, M. L.; Shin, K.; Coggin, D. K.; Hagen, P. A.; Huffman, J. C.; Christou, G.; Hendrickson, D. N. *J. Am. Chem. Soc.* **1991**, *113*, 3012–3021. (b) Sessler, J. L.; Hugdahl, J. D.; Lynch, V.; Davis, B. *Inorg. Chem.* **1991**, *30*, 334–336. (c) Nishida, Y.; Nasu, M.; Tokii, T. *Z. Naturforsch.* **1990**, *45b*, 567–570. (d) Sessler, J. L.; Sibert, J. W.; Lynch, V. *Inorg. Chem.* **1990**, *29*, 4143–4146. (e) Drueke, S.; Wieghardt, K.; Nuber, B.; Weiss, J.; Bominaar, E. L.; Sawaryn, A.; Winkler, H.; Trautwein, A. X. *Inorg. Chem.* **1989**, *28*, 4477–4483. (f) Chen, Q.; Lynch, J. B.; Gomez-Romero, P.; Ben-Hussein, A.; Jameson, G. B.; O'Connor, C. J.; Que, L., Jr. *Inorg. Chem.* **1988**, *27*, 2673–2681. (g) Gorun, S. M.; Lippard, S. J. *Inorg. Chem.* **1988**, *27*, 149–156. (h) Murch, B. P.; Bradley, F. C.; Boyle, P. D.; Papaefthymiou, V.; Que, L., Jr. *J. Am. Chem. Soc.* **1987**, *109*, 7993–8003. (i) Armstrong, W. H.; Roth, M. E.; Lippard, S. J. *J. Am. Chem. Soc.* **1987**, *109*, 6318–6326. (j) Jameson, D. L.; Xie, C. L.; Hendrickson, D. N.; Potenza, J. A.; Schugar, H. J. *J. Am. Chem. Soc.* **1987**, *109*, 740–746. (k) Toftlund, H.; Murray, K. S.; Zwack, P. R.; Taylor, L. F.; Anderson, O. P. *J. Chem. Soc., Chem. Commun.* **1986**, 191–193. (l) Turte, K. I.; Bobkova, S. A.; Kuyavskaya, B. Y.; Ivleva, I. N.; Ponomarev, V. I.; Veksel'man, M. E. *Koord. Khim.* **1985**, *11*, 1106–1112. (m) Sessler, J. L.; Sibert, J. W.; Lynch, V.; Markert, J. T.; Wooten, C. L. *Inorg. Chem.* **1993**, *32*, 621–626.

0020-1669/93/1332-4277$04.00/0

exhibit a vast array of geometries within their iron cores. Recent efforts by our group[11b,d,m] and others[11k] have shown that ditopic ligands in which the two binding sites are covalently-linked via a tether devoid of any potential ligating functionality apparently discourage the formation of hemerythrin (Hr)-like, (μ-oxo)bis(μ-carboxylato)diiron(III) complexes. Instead, a tetranuclear iron(III) complex having a "dimer of Hr-like dimers" structure is formed.

In an effort to stabilize the dinuclear structure, we have synthesized the new heptadentate ligand 1,3-bis(1,4,7-triaza-1-cyclononyl)-2-hydroxypropane (dtnp-OH). The ligand is composed of two macrocyclic tridentate capping moieties covalently linked by a three-carbon bridge which contains a hydroxyl functionality as a potential seventh donor group. Interestingly, in either the presence or absence of a carboxylate source, the ligand stabilizes a tetranuclear iron(III) complex in which the Fe_4O_6 core has an adamantane-like geometry and contains no carboxylate ligands.

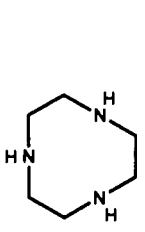

TACN

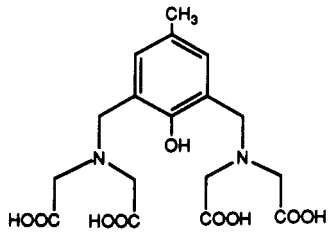

5-Me-HXTA

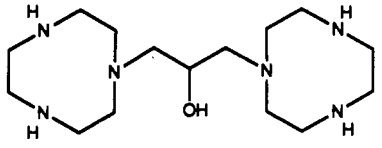

dtnp-OH

To our knowledge, there are only two related tetranuclear iron–oxo clusters in the literature. Que et al. have reported the synthesis in basic media of $(L_2Fe_4(O)_2(OH)_2)^{4+}$ (L = *N,N'*-2-hydroxy-5-*R*-1,3-xylylenebis(*N*-carboxymethyl)glycine (5-Me-HXTA)).[11h] The tetranuclear complex was found to be in a pH-dependent equilibrium with a dinuclear iron(III) complex, $LFe_2(OH)(H_2O)_2$. More recently, Wieghardt et al. have synthesized $(L'_4Fe_4(O)_2(OH)_4)^{4+}$ (L' = 1,4,7-triazacyclononane (TACN)) under neutral to basic conditions.[11e]

We report here the syntheses and physical properties of both ligand dtnp-OH (**2**) and the tetranuclear iron(III) complex **4**, $C_{36}H_{86}N_{12}O_{10}P_4F_{24}Fe_4$, which it stabilizes.

Experimental Section

Materials and Apparatus. The reagent 1,3-dibromo-2-propanol was obtained from Tokyo Kasei. *N,N'*-bis(*p*-tolylsulfonyl)-1,4,7-triazacyclononane was prepared according to literature procedures.[11d,16] All other reagents and solvents were of reagent grade quality, obtained from commercial suppliers, and used without further purification. Proton and carbon NMR spectra were recorded on a General Electric QE-300 (300 MHz) spectrometer. Electronic spectra were recorded on a Beckman DU-7 spectrophotometer. Fourier transform infrared spectra were obtained on a Bio-Rad FTS-40 spectrophotometer. Elemental analysis was performed by Atlantic Microlab.

Preparation of 1,3-Bis[*N,N'*-bis(*p*-tolylsulfonyl)-1,4,7-triaza-1-cyclononyl]-2-hydroxypropane (1). A solution containing *N,N'*-bis(*p*-tolylsulfonyl)-1,4,7-triazacyclononane (2.42 g; 5.54 mmol), 1,3-dibromo-2-propanol (283 μL; 2.77 mmol), and triethylamine (1 mL) in acetonitrile (100 mL) was stirred and heated at reflux under a nitrogen atmosphere for 24 h. The solvent was then removed on a rotary evaporator. The residue was taken up in $CHCl_3$, and the solution was washed with 1 N NaOH. The organic layer was dried over $MgSO_4$. Pure **1** was obtained as a white solid (1.74 g) following column chromatography on silica (2% $CH_3OH/CHCl_3$): yield 68%; mp 102–107 °C; ^{1}H NMR δ 1.68 (1 H, br, O*H*), 2.40 (12 H, s, CH_3Ar), 2.55 (2 H, dd, NC(H_a)H_bC(H)OH)), 2.76 (2 H, dd, NC(H_a)H_bC(H)OH)), 3.01 (8 H, t, TsNCH_2-CH_2N(CH_2)$_2$), 3.23 (8 H, br, TsNCH_2CH_2N(CH_2)$_2$), 3.45 (8 H, br, TsNCH_2CH_2NTs), 3.80 (1 H, quintet, NCH_2C(*H*)OHCH_2N), 7.28 (8 H, d, aromatic), 7.64 (8 H, d, aromatic); ^{13}C NMR δ 21.30, 52.03, 52.74, 56.33, 62.61, 67.44, 126.99, 129.58, 135.01, 143.26; CI MS *m/e* 932 (MH^+), 776 (M - Ts).

Preparation of 1,3-Bis(1,4,7-triaza-1-cyclononyl)-2-hydroxypropane (2). Compound **1** (1.40 g, 1.50 mmol), anhydrous disodium phosphate (2 g), and 2% Na amalgam (42 g) were placed in 25 mL of dry methanol. The mixture was heated at reflux under N_2 for 20 h while stirring rapidly. After being cooled to room temperature, the resulting slurry was decanted into water and extracted three times with chloroform. The organic layers were combined and dried over $MgSO_4$. The $MgSO_4$ was filtered out and the solvent removed *in vacuo* to yield **2** (384 mg) as a white solid: yield 81%; IR ($CHCl_3$, cm^{-1}, selected peaks) 3324 (m), 3247 (m), 2874 (w), 2930 (w), 2853 (m), 1480 (w), 1104 (s), 932 (vs), 741 (vs), 683 (vs); ^{1}H NMR ($CDCl_3$) δ 2.29–2.58 (m), 2.58–2.70 (m), 2.73–3.21 (m), 3.50 (br), 3.63 (br), 3.78 (t), 3.88 (br), 6.40 (1 H, br, O*H*); ^{13}C NMR ($CDCl_3$) δ 41.04, 41.08, 41.57, 41.84, 45.73, 45.84, 47.03, 47.27, 49.35, 49.64, 55.71, 56.07, 65.04, 65.29, 67.49; ^{13}C NMR (D_2O/CF_3COOD (1:1)) δ 45.44, 47.15, 51.40, 62.53, 69.21; CI MS *m/e* 315 (MH^+); HR EI MS *m/e* 315.2884 (MH^+) (calcd for $C_{15}H_{35}N_6O_1$, m/e 315.2872), m/e 314.2784 (M^+) (calcd for $C_{15}H_{34}N_6O_1$, *m/e* 314.2794).

Preparation of $[2(Fe_2(O)(OH))]_2X_4$ (4X; X = PF_6, BF_4). Method a. To a solution of **2** (66.0 mg) in isopropyl alcohol (25 mL) was added $FeCl_3{\cdot}6H_2O$ (113.6 mg). The resulting hygroscopic yellow precipitate, **3**, was collected by filtration, and washed first with isopropyl alcohol and then ethyl ether. To a suspension of complex **3** in ethanol (50 mL) was added excess sodium acetate (or sodium benzoate), triethylamine, and potassium hexafluorophosphate. The resulting gold-colored solution was stirred at room temperature for 24–36 h (until the formation of a green precipitate was observed). The precipitate was isolated by filtration. It was then taken up in acetone and filtered to remove white solids, presumably NaCl and KCl. The acetone was removed on a rotary evaporator to leave a green solid. Dark green, needle-shaped crystals of **4** were grown by diffusion of methanol into an acetonitrile solution containing this green solid. X-ray-quality crystals were obtained by the slow evaporation of an acetone/IPA solution containing **4**.

Method b. Using the same procedure as in method a, with the exclusion of any carboxylate source, **4** was produced as a green precipitate in 2–4 days. Purification was as described above.

Method c. Under an argon atmosphere, **2** (76.4 mg) and $FeBF_4{\cdot}4H_2O$ (146.0 mg) were added to 30 mL of dry, degassed methanol. After the mixture was stirred for 1 h, sodium benzoate (35 mg) was added and the solution color changed from colorless to yellow. Stirring was continued at room temperature for an additional 6 h. At this time, the solvent was removed by evaporation and the residue taken up in acetonitrile. The acetonitrile solution was filtered, and golden-brown crystals were then obtained by diffusion of ethyl ether into the acetonitrile filtrate. Bubbling air through an acetonitrile solution containing this Fe(II) complex caused a gradual solution color change (from yellow to green) over the course of several hours. Green crystals which have the same spectroscopic properties as **4** (prepared from method a or b) were then grown by evaporation of the green acetonitrile solution: IR (KBr, cm^{-1}, selected

(12) (a) Nair, V. S.; Hagen, K. S. *Inorg. Chem.* **1992**, *31*, 4048–4050. (b) Hegetschweiler, K.; Schmalle, H. W.; Streit, H. M.; Gramlich, V.; Hund, H. U.; Erni, I. *Inorg. Chem.* **1992**, *31*, 1299–1302. (c) McCusker, J. K.; Christmas, C. A.; Hagen, P. M.; Chadha, R. K.; Harvey, D. F.; Hendrickson, D. N. *J. Am. Chem. Soc.* **1991**, *113*, 6114–6124. (d) Micklitz, W.; Bott, S. G.; Bentsen, J. G.; Lippard, S. J. *J. Am. Chem. Soc.* **1989**, *111*, 372–374. (e) Micklitz, W.; Lippard, S. J. *Inorg. Chem.* **1988**, *27*, 3067–3069. (f) Batsanov, A. S.; Struchkov, Y. T.; Timko, G. A. *Koord. Khim.* **1988**, *14*, 266–270.

(13) Wieghardt, K.; Pohl, K.; Jibril, I.; Huttner, G. *Angew. Chem., Int. Ed. Engl.* **1984**, *23*, 77–78.

(14) Taft, K. L.; Lippard, S. J. *J. Am. Chem. Soc.* **1990**, *112*, 9629–9630.

(15) (a) Gorun, S. M.; Papaefthymiou, G. C.; Frankel, R. B.; Lippard, S. J. *J. Am. Chem. Soc.* **1987**, *109*, 3337–3348. (b) Taft, K. L.; Papefthymiou, G. C.; Lippard, S. J. *Science* **1993**, *259*, 1302–1305. (c) Heath, S. L.; Powell, A. K. *Angew. Chem., Int. Ed. Engl.* **1992**, *31*, 191–193.

(16) Wieghardt, K.; Tolksdorf, I.; Herrmann, W. *Inorg. Chem.* **1985**, *24*, 1230–1235.

Table I. Crystallographic Data for $4(PF_6)_4 \cdot 2H_2O \cdot 2C_2H_6O$

chem formula	$C_{36}H_{86}N_{12}O_{10}P_4F_{24}Fe_4$
a, Å	15.360(3)
b, Å	16.150(3)
c, Å	25.225(3)
V, Å^3	6257(2)
Z	4
fw	1650.39
space group	$P2_12_12_1$ (No. 19)
T, °C	−100
λ(Mo Kα), Å	0.7107
ρ_{calc}, g/cm^3 (−100 °C)	1.75
μ, cm^{-1}	11.37
$R(F)^a$	0.0618
$R_w(F)$	0.0668

^{a} $R(F) = \sum(|F_o| - |F_c|)/F_o$; $R_w(F) = \sum w(|F_o| - |F_c|^2/w(|F_o|)^2$, where $w = 1/(\sigma(F_o)^2 + (0.02F)^2)$.

peaks) 3607 (m), 3339 (s), 2926 (m), 1463 (m), 1104 (s), 1009 (s), 837 (vs), 798 (s), 768 (s), 736 (m), 652 (m), 559 (vs), 516 (m); UV–vis (ε, M^{-1} cm^{-1}/Fe) 455 (sh), 481 (261), 613 (100). Anal. Calcd for $C_{30}H_{68}N_{12}O_6Fe_4P_4F_{24}$: C, 24.08; H, 4.58; N, 11.23. Found: C, 24.56; H, 4.44; N, 11.51. Complex **4** was further characterized by X-ray crystallography.

X-ray Crystallography. The data crystal was a green prism of approximate dimensions 0.2 × 0.3 × 0.6 mm. The data were collected at −100 °C on a Nicolet R3 diffractometer, with a graphite monochromator using Mo Kα radiation (λ = 0.7107 Å) and equipped with a Nicolet LT-2 low-temperature delivery system. The hexafluorophosphate complex of **4** crystallized with two molecules of H_2O and two molecules of acetone in the unit cell. Details of crystal data and refinement are listed in Table I. The lattice parameters were obtained from least-squares refinement of 40 reflections with $20.0 < 2\theta < 25.0°$. The data were collected using the Ω scan technique from 4 to 50° in 2θ, with a scan width of 1.2° and a scan rate of 3–6°/min. A total of 6815 reflections were collected, of which 6113 were unique (h ranged from 0 to 19; k from 0 to 20; l from 0 to 30). The R for averaging equivalent reflections was 0.026. Four reflections (4,–6,8; 3,7,8; 3,–7,8; 4,–6,–8) were remeasured every 96 reflections to monitor instrument and crystal stability. A smoothed curve of the intensities of these check reflections was used to scale the data. The scaling factor ranged from 0.963 to 1.05. The data were also corrected for Lp effects but not for absorption. Crystal faces could not be completely indexed, and, therefore an absorption correction was not applied. Reflections having $F_o < 4(\sigma(F_o))$ were considered unobserved (1327 reflections). The structure was solved by direct methods and refined by full-matrix least-squares procedures with anisotropic thermal parameters for the non-hydrogen atoms. The structure was refined in blocks of 406 and 397 parameters, respectively, with an overall scale factor and the atoms of the disordered PF_6^- group refined in each block. Most hydrogens were calculated in idealized positions (C–H = 0.96 Å, N–H = 0.90 Å) with an isotropic thermal parameter fixed at $1.2U_{eq}$ of the relevant atom. Three H atoms bound to oxygen atoms, two for hydroxy oxygens, O12 and O34, and one from a water oxygen, O1C, were obtained from a ΔF map but fixed during refinement with U_{iso} fixed. One of the PF_6^- groups was found to be disordered about two principle orientations by rotation about the P atom, P4. The site occupation factor for the major component refined to 57.7(7)%. The atoms of the minor component have labels appended with A (F19A–F24A). The disordered F's were refined with isotropic thermal parameters. A total of 781 independent parameters were refined. The data were checked for secondary extinction errors which were found to be insignificant. The function, $\sum w(|F_o| - |F_c|)^2$, was minimized, where $w = 1/(\sigma(F_o))^2$ and $\sigma(F_o) = 0.5kI^{-1/2}[(\sigma(I))^2 + (0.02I)^2]^{1/2}$. The intensity, I, is given by (Ipeak − I_{bkgd}) × (scan rate), 0.02 is a factor to downweight intense reflections and to account for instrument instability, and k is the correction due to Lp effects and decay. $\sigma(I)$ was estimated from counting statistics; $\sigma(I) = [(I_{peak} + I_{bkgd})^{1/2} \times$ (scan rate)]. Final $R = 0.0618$ for 4786 reflections, $R_w = 0.0668$ (R for all reflections = 0.0817, R_w for all reflections = 0.0696), and goodness of fit = 1.940. The maximum |shift/esd| < 0.1 in the final refinement cycle, and the minimum and maximum peaks in the final difference electron density map were −0.66 and 1.09 e/Å^3 (near the disordered PF_6^- group), respectively. The absolute configuration of the structure was assigned by the η refinement method. The multiplicity factor for $\Delta f''$ refined to 0.98(7) indicating the correct absolute configuration as given. The structure solution and refinement were done using SHELXTL-Plus.[17] The scattering factors for the non-H atoms were taken from Cromer and Mann,[18] with anomalous-dispersion corrections from Cromer and Liberman,[19] while scattering factors for the H atoms were obtained from Stewart, Davidson, and Simpson.[20] The linear absorption coefficient was calculated from values in ref 21. Other computer programs were from ref 11 of Gadol and Davis.[22]

Magnetic Susceptibility Measurements. Solid-state magnetic susceptibilities of a powdered sample of **4** were measured between 2 and 300 K at a field of 10 kG using a Quantum Design Model MPMS SQUID magnetometer. A total of 73 data points were measured. The susceptibilities were corrected for the magnetism of the quartz sample holder. Gram susceptibilities were converted to molar susceptibilities and then corrected for diamagnetism ($\chi_d = -719 \times 10^{-6}$ cgs/mol) using Pascal's constants.[23]

Results and Discussion

Ligand Synthesis. As shown in Scheme I, the reaction of 2 equiv of *N,N'*-bis(*p*-tolylsulfonyl)-1,4,7-triazacyclononane with 1,3-dibromo-2-propanol in the presence of triethylamine produces the protected bis(TACN)[24] ligand **1** in good yield. The acidic conditions needed to remove the tosyl protecting groups (e.g. concentrated H_2SO_4, 100 °C, 2 days or HBr/AcOH, 90°C, 36 h) were considered to be too harsh to use in the presence of the secondary alcohol. Consequently, a reductive detosylation procedure (2% Na/Hg) was used to produce **2** in greater than 75% yield.[25]

Characterization of **2** was complicated by the presence of inter- and/or intramolecular hydrogen-bonding interactions. These H-bonding interactions are not seen in other bis(TACN) ligands which lack the alcohol functionality on the hydrocarbon tether.[11d,16] The ^{1}H NMR and ^{13}C NMR spectra of **2** in $CDCl_3$ do not, thus, reflect the C_2 symmetry expected for the molecule.

More specifically, the proton NMR spectrum of **2** in $CDCl_3$ exhibits a broad band of resonances between 2.3 and 3.9 ppm. No resonances in the aromatic region were observed, indicating that complete detosylation had occurred. When the spectrum is taken in more polar solvents, such as CD_3OD or D_2O, a broad band of unresolved resonances is still observed between 2.5 and 3.5 ppm. Variable-temperature proton ^{1}H NMR spectra were recorded in DMSO at room temperature, 60 °C, and 90 °C. While subtle changes were observed, little improvement in resolution occurred. Hence, **2** could not be characterized completely using this method.

Because decoupled ^{13}C NMR spectra seldom have overlapping resonances, the H-bonding interactions in **2** are more easily monitored by ^{13}C NMR. As shown in Figure 1, the ^{13}C NMR spectrum of **2** in $CDCl_3$ shows a resonance for nearly every carbon in the molecule, reflecting the asymmetry of the molecule. When the ^{13}C NMR spectrum is taken in a more polar environment, D_2O/CF_3COOD (1:1), however, only five carbon resonances are observed. Under these conditions, the H-bonding interaction is broken and the molecule displays its full C_2 symmetry. The ligand was further characterized by high-resolution mass spectrometry.

Metal Complex Formation. As shown in Scheme II, three different metalation pathways involving ligand **2** were used to form the same iron(III) complex.

(17) SHELXTL-*PLUS*; Siemens Analytical X-ray Instruments, Inc.: Madison, WI, 1990.
(18) Cromer, D. T.; Mann, J. B. *Acta Crystallogr.* **1968**, *A24*, 321–324.
(19) Cromer, D. T.; Liberman, D. *J. Chem. Phys.* **1970**, *53*, 1891–1898.
(20) Stewart, R. F.; Davidson, E. R.; Simpson, W. T. *J. Chem. Phys.* **1965**, *42*, 3175–3187.
(21) *International Tables for X-ray Crystallography*; Kynoch: Birmingham, England, 1974; Vol. IV, p 55.
(22) Gadol, S. M.; Davis, R. E. *Organometallics* **1982**, *1*, 1607–1613.
(23) Carlin, R. L. In *Magnetochemistry*; Springer-Verlag: Berlin, **1986**; p 3.
(24) "Bis(macrocycle)" is defined as a molecule composed of two covalently-linked macrocycles: Ciampolini, M.; Fabbrizzi, L.; Perotti, A.; Poggi, A.; Seghi, B.; Zanobini, F. *Inorg. Chem.* **1987**, *26*, 3527–3533.
(25) Sessler, J. L.; Sibert, J. W.; Hugdahl, J. D.; Lynch, V. *Inorg. Chem.* **1989**, *28*, 1417–1419.

Table II. Fractional Coordinates and Equivalent Isotropic Thermal Parameters (Å^2) for the Non-Hydrogen Atoms of $4(PF_6)_4 \cdot 2H_2O \cdot 2C_2H_6O$

atom	x	y	z	U^a	atom	x	y	z	U^a
Fe1	0.64050(10)	0.09443(9)	0.87017(5)	0.0236(4)	C41	0.5462(7)	−0.0902(8)	1.0083(4)	0.048(4)
Fe2	0.74986(10)	−0.07254(9)	0.81108(5)	0.0209(4)	N42	0.5995(6)	−0.1425(6)	0.9737(4)	0.040(3)
Fe3	0.86551(10)	0.05933(9)	0.88552(5)	0.0221(4)	C43	0.6260(8)	−0.2207(7)	0.9980(5)	0.045(4)
Fe4	0.70665(10)	−0.06314(10)	0.94786(5)	0.0272(5)	C44	0.7212(9)	−0.2378(7)	0.9870(5)	0.049(5)
O13	0.7629(4)	0.1330(4)	0.8765(2)	0.026(2)	O1C	0.7663(6)	0.2966(6)	0.9218(3)	0.059(3)
O14	0.6440(5)	0.0204(4)	0.9232(3)	0.030(2)	O1D	0.5721(9)	−0.2395(8)	0.8684(5)	0.121(6)
O23	0.8440(5)	−0.0128(4)	0.8312(3)	0.027(2)	P1	0.2402(2)	−0.7229(2)	0.93946(12)	0.0384(10)
O24	0.7171(5)	−0.1257(4)	0.8785(3)	0.030(2)	F1	0.1723(5)	−0.6641(5)	0.9103(3)	0.068(3)
N1	0.6042(6)	0.1850(5)	0.8065(3)	0.033(3)	F2	0.1638(5)	−0.7708(6)	0.9692(3)	0.076(3)
C2	0.6174(8)	0.2682(7)	0.8300(4)	0.040(4)	F3	0.3090(5)	−0.7806(4)	0.9696(3)	0.051(3)
C3	0.5710(8)	0.2741(6)	0.8822(4)	0.039(4)	F4	0.3168(6)	−0.6769(8)	0.9142(4)	0.129(5)
N4	0.5898(6)	0.1983(6)	0.9152(3)	0.036(3)	F5	0.2437(6)	−0.6615(5)	0.9898(3)	0.074(3)
C5	0.5110(8)	0.1665(8)	0.9416(5)	0.043(4)	F6	0.2355(8)	−0.7821(7)	0.8917(3)	0.115(5)
C6	0.4501(8)	0.1259(8)	0.9009(5)	0.046(4)	P2	0.5416(3)	−0.4636(3)	0.87689(14)	0.0553(13)
N7	0.4998(5)	0.0753(6)	0.8624(3)	0.031(3)	F7	0.6194(6)	−0.4068(7)	0.8576(4)	0.108(5)
C8	0.4762(7)	0.0901(7)	0.8071(5)	0.039(4)	F8	0.5366(7)	−0.4082(6)	0.9284(3)	0.097(4)
C9	0.5138(7)	0.1711(7)	0.7886(5)	0.038(4)	F9	0.4663(6)	−0.5207(6)	0.8970(4)	0.097(4)
C10	0.6704(8)	0.1654(7)	0.7663(4)	0.038(4)	F10	0.5445(7)	−0.5187(7)	0.8262(4)	0.115(5)
C11	0.6703(7)	0.0711(6)	0.7563(4)	0.027(3)	F11	0.6103(7)	−0.5224(6)	0.9028(5)	0.124(5)
O12	0.6679(4)	0.0288(4)	0.8055(2)	0.021(2)	F12	0.4764(7)	−0.4073(6)	0.8501(4)	0.107(5)
C13	0.7535(7)	0.0492(7)	0.7256(4)	0.034(4)	P3	0.0457(3)	−0.2884(2)	0.81916(13)	0.0505(12)
N14	0.7615(6)	−0.0420(5)	0.7258(3)	0.028(3)	F13	0.1189(6)	−0.2690(7)	0.8607(3)	0.098(4)
C15	0.8494(7)	−0.0687(7)	0.7106(4)	0.034(4)	F14	0.0627(6)	−0.3849(5)	0.8275(3)	0.081(4)
C16	0.8645(8)	−0.1571(7)	0.7258(4)	0.039(4)	F15	−0.0258(6)	−0.3100(5)	0.7757(3)	0.078(3)
N17	0.8291(6)	−0.1751(5)	0.7818(3)	0.028(3)	F16	0.0282(5)	−0.1913(5)	0.8093(3)	0.064(3)
C18	0.7775(7)	−0.2520(7)	0.7883(5)	0.040(4)	F17	−0.0292(6)	−0.2875(6)	0.8624(3)	0.098(4)
C19	0.6902(7)	−0.2430(7)	0.7622(5)	0.040(4)	F18	0.1167(5)	−0.2886(6)	0.7733(3)	0.085(4)
N20	0.6519(6)	−0.1593(5)	0.7735(3)	0.034(3)	O1A	0.3933(8)	0.0587(7)	1.0412(5)	0.100(5)
C21	0.6179(7)	−0.1158(7)	0.7257(4)	0.035(4)	C2A	0.3342(12)	0.0049(11)	1.0410(7)	0.081(7)
C22	0.6944(7)	−0.0825(7)	0.6939(4)	0.037(4)	C3A	0.2620(13)	0.0106(14)	1.0023(7)	0.112(9)
N23	0.9935(6)	0.0085(6)	0.9084(3)	0.031(3)	C4A	0.3404(14)	−0.0663(11)	1.0814(9)	0.129(10)
C24	1.0342(7)	0.0554(7)	0.9539(4)	0.036(4)	O1B	0.7816(13)	−0.5958(11)	0.8381(5)	0.205(11)
C25	0.9693(7)	0.1106(7)	0.9818(4)	0.034(4)	C2B	0.813(2)	−0.566(2)	0.7987(9)	0.124(11)
N26	0.9157(5)	0.1549(5)	0.9433(3)	0.030(3)	C3B	0.9060(14)	−0.5544(14)	0.7954(8)	0.133(10)
C27	0.9643(7)	0.2232(7)	0.9156(4)	0.036(4)	C4B	0.768(2)	−0.505(2)	0.7692(11)	0.20(2)
C28	0.9510(8)	0.2196(7)	0.8561(4)	0.040(4)	P4	0.3648(4)	−0.1328(3)	0.8672(2)	0.154(4)
N29	0.9558(6)	0.1331(5)	0.8375(3)	0.031(3)	F19A	0.4564(4)	−0.1074(3)	0.8907(2)	0.142(11)
C30	1.0454(7)	0.0988(8)	0.8375(4)	0.041(4)	F20A	0.3310(4)	−0.1524(3)	0.9251(2)	0.50(6)
C31	1.0465(7)	0.0112(7)	0.8584(4)	0.035(4)	F21A	0.2731(4)	−0.1582(3)	0.8439(2)	0.25(2)
C32	0.9715(7)	−0.0777(7)	0.9227(4)	0.040(4)	F22A	0.3985(4)	−0.1131(3)	0.8095(2)	0.084(7)
C33	0.8961(7)	−0.0770(7)	0.9620(4)	0.033(4)	F23A	0.3324(4)	−0.0403(3)	0.8731(2)	0.117(11)
O34	0.8321(4)	−0.0223(4)	0.9444(2)	0.026(2)	F24A	0.3971(4)	−0.2252(3)	0.8614(2)	0.070(6)
C35	0.8599(8)	−0.1654(7)	0.9685(5)	0.040(4)	F19	0.3294(4)	−0.0458(3)	0.8483(2)	0.196(13)
N36	0.7743(7)	−0.1612(6)	0.9943(4)	0.041(4)	F20	0.4524(4)	−0.1170(3)	0.8361(2)	0.28(2)
C37	0.7818(9)	−0.1386(8)	1.0512(4)	0.047(5)	F21	0.4002(4)	−0.2197(3)	0.8862(2)	0.63(6)
C38	0.7611(9)	−0.0484(8)	1.0604(5)	0.056(5)	F22	0.2771(4)	−0.1485(3)	0.8984(2)	0.142(8)
N39	0.6850(6)	−0.0209(6)	1.0293(3)	0.036(3)	F23	0.4053(4)	−0.0908(3)	0.9182(2)	0.158(9)
C40	0.6015(9)	−0.0522(9)	1.0509(5)	0.056(5)	F24	0.3242(4)	−0.1747(3)	0.8163(2)	0.33(2)

[a] For anisotropic atoms, the U value is U_{eq}, calculated as $U_{eq} = {}^1/_3\sum_i\sum_j U_{ij}a_ia_jA_{ij}$, where A_{ij} is the dot product of the ith and jth direct space unit cell vectors.

The reaction of **2** with 2 equiv of $FeCl_3 \cdot 6H_2O$ in isopropyl alcohol produced a hygroscopic, mustard yellow solid, **3**, presumed to be the 2:1 metal-to-ligand complex. This solid was then suspended in an ethanol solution containing triethylamine, 2 equiv of either sodium acetate or sodium benzoate, and potassium hexafluorophosphate. Under similar conditions, hemerythrin (Hr) -model complexes, containing the familiar (μ-oxo)bis(μ-carboxylato)diiron(III) core, are known to self-assemble readily from a variety of ligands, including bis(TACN) systems in which there is no ligating functionality on the tether.[11d,m,16] After stirring of the mixture at room temperature for 1 h, the reaction consisted of a golden brown-colored solution and a white precipitate (NaCl, KCl and/or unreacted NaOAc, NaOBz). As judged by visible spectroscopy, no Hr-like diiron(III) core was present in the solution. The reaction was allowed to stir for approximately 24 h at which time a green precipitate had formed. This precipitate, $4(PF_6)_4$, is soluble in both acetone and acetonitrile and produces green solutions. Diffusion of methanol into an acetonitrile solution containing $4(PF_6)_4$ produces dark green, needle-shaped crystals. The visible spectrum, taken in acetonitrile, displays two distinctive features, a weak absorption at 613 nm (ϵ = 100 M^{-1} cm^{-1}/Fe) and a shoulder at 481 nm (ϵ = 261 M^{-1} cm^{-1}/Fe) to a much larger absorption that extends into the UV region. The spectrum is nearly identical to that reported for Wieghardt's tetranuclear iron(III) complex which lacks any carboxylate ligands and contains the adamantane-like $Fe_4(O)_2(OH)_4$ core.[11e] Additionally, the IR spectrum of $4(PF_6)_4$ lacks characteristic symmetric and asymmetric carboxylate stretches.

Since the evidence indicates that there are no bridging carboxylates present in **4**, its synthesis was attempted using the same method as just described without the addition of any carboxylate source to **3**. In this case, a green precipitate, identified spectroscopically as **4**, also formed, though, under these conditions, the required reaction time was several days.

A third pathway for the synthesis of **4** begins with the reaction of **2** and 2 equiv of $Fe(BF_4)_2 \cdot 4H_2O$ in methanol under an argon atmosphere. Following the addition of sodium benzoate, the solution turned yellow. The solvent was removed and the resulting golden-brown solid taken up in acetonitrile. Following filtration to remove NaCl and unreacted NaOBz, brown crystals were grown by vapor diffusion of ether into the acetonitrile filtrate containing the iron(II) complex. At room temperature, dioxygen was bubbled through an acetonitrile solution containing this putative iron(II) complex. The solution color gradually changed from yellow to

Table III. Selected Mean Bond Angles (deg) and Distances (Å) for Complex **4**

	Bond Lengths		
Fe1–O12	1.989(6)	Fe1–O13	1.987(7)
Fe1–O14	1.796(7)	Fe2–O12	2.070(6)
Fe2–O23	1.811(7)	Fe2–O24	1.971(7)
Fe3–O13	1.988(7)	Fe3–O23	1.828(7)
Fe3–O34	2.051(7)	Fe4–O14	1.770(7)
Fe4–O24	2.026(7)	Fe4–O34	2.039(7)
Fe1–N1	2.242(9)	Fe1–N4	2.170(9)
Fe1–N7	2.192(8)	Fe2–N14	2.215(8)
Fe2–N17	2.185(8)	Fe2–N20	2.264(9)
Fe3–N23	2.207(9)	Fe3–N26	2.258(9)
Fe3–N29	2.193(9)	Fe4–N36	2.227(10)
Fe4–N39	2.191(8)	Fe4–N42	2.185(10)
Fe1···Fe2	3.510(2)	Fe1···Fe3	3.524(2)
Fe1···Fe4	3.369(3)	Fe2···Fe3	3.350(2)
Fe2···Fe4	3.517(2)	Fe3···Fe4	3.513(2)
	Bond Angles		
Fe1–O12–Fe2	119.6(3)	Fe1–O13–Fe3	124.9(3)
Fe1–O14–Fe4	141.7(4)	Fe2–O23–Fe3	134.0(4)
Fe2–O24–Fe4	123.3(3)	Fe3–O34–Fe4	118.4(3)

Scheme I

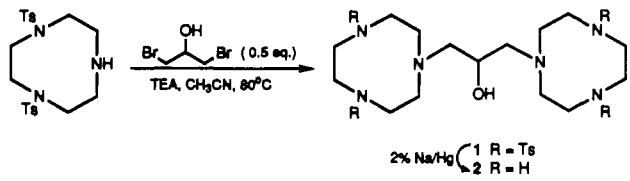

green. The green-colored product was spectroscopically identical to the original system, **4**$(PF_6)_4$. Thus, the material produced in this manner was judged to contain the same iron complex, **4**, as that obtained directly from iron(III) sources.

Description of the Structure. Green, X-ray-quality, crystals of **4**$(PF_6)_4$, produced from method a, were grown by slow evaporation of an acetone/isopropyl alcohol solution. The structure consists of a quadruply-charged, tetranuclear iron(III) cation (Figure 2) and four hexafluorophosphate anions. The Fe_4O_6 core is composed of a tetrahedron of iron atoms which are bridged by six oxygen atoms (two oxo groups (O14 and O23, bridging Fe1 and Fe4 and Fe2 and Fe3, respectively), two hydroxo groups (O13 and O14, bridging Fe1 and Fe3 and Fe1 and Fe4, respectively), and two alkoxo groups from two molecules of ligand **2** (O12 and O34, bridging Fe1 and Fe2 and Fe3 and Fe4, respectively)). This results in an adamantane-like geometry with the iron atoms occupying the bridgehead positions (Figure 3). The Fe_4O_6 core is capped by two molecules of **2** which act as ditopic, heptadentate ligands.

Each of the four iron atoms lies at the center of a distorted octahedral coordination environment comprising one facially-coordinating triazacyclononane ring, one μ-oxo ligand, one μ-hydroxo ligand, and one μ-alkoxo ligand. The four triazacyclononane rings exhibit two slightly different coordination geometries. The donor atoms which are coordinated trans to the oxo ligand, O14, at Fe1 and Fe4 are macrocyclic *tertiary* amines (N1 and N36, respectively), whereas the donor atoms trans to the oxo ligand, O23, at Fe2 and Fe3 are macrocyclic *secondary* amines (N20 and N26, respectively). The net effect is that the two TACN rings coordinated to Fe2 and Fe3 are rotated with respect to the two TACN rings attached to Fe1 and Fe4.

Interestingly, unlike the 5-Me-HXTA complex of Que et al.,[11h] there is a trans effect exhibited by the oxo-bridges on each of the four iron atoms of **4**. This effect is also seen in the $Fe_4(O)_2(OH)_4$ core synthesized by Wieghardt et al.[11e] The result of this trans effect, which is common in oxo-bridged iron(III) complexes,[9] is a lengthening of the Fe–N bond trans to the oxo bridge (average = 2.248(5) Å) relative to the Fe–N bonds cis to the oxo bridge (average = 2.192(3) Å).

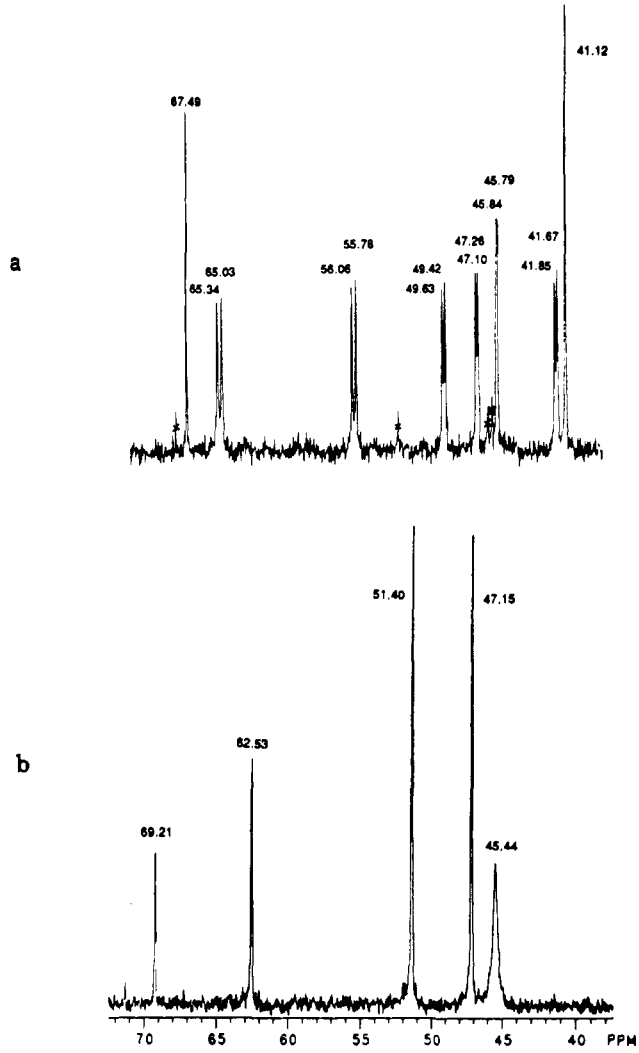

Figure 1. (a) Decoupled ^{13}C NMR spectrum of **2** in $CDCl_3$. Peaks marked with an "×" derive from impurities. (b) Decoupled ^{13}C NMR spectrum of **2** in D_2O/CF_3COOD (1:1).

Scheme II

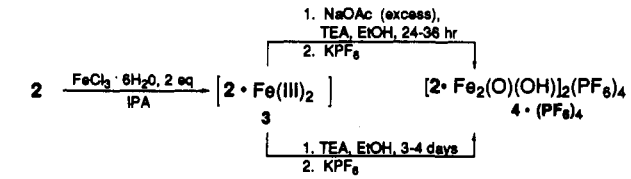

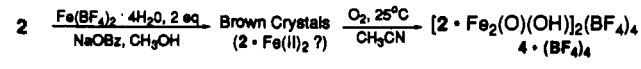

The presence of three different types of bridging oxygen atoms (alkoxo, O12 and O34, hydroxo, O13 and O24, and oxo, O14 and O23) allows for a comparison of their respective bonding characteristics. The average length of the Fe–OH bonds (1.993(4) Å) is similar to that of the Fe–OC bonds (2.037(3) Å) but much longer than that of the Fe–O bonds (1.801(7) Å). These distances are typical for each type of bond and reflect the increased π character in the Fe–O bond. The Fe···Fe distances are nearly identical for the iron atoms bridged by hydroxo and alkoxo ligands (average = 3.516(1) Å), which, in turn, are longer than the corresponding oxo-mediated Fe···Fe distances (average = 3.360(2) Å). Notably, the Fe–O–Fe bond angle (average = 137.9(3)°) is significantly larger than either the Fe–OH–Fe bond angle (average = 124.1(2)°) or the Fe–OC–Fe bond angle (average = 119.0(2)°). The widening of the Fe–O–Fe bond angle appears

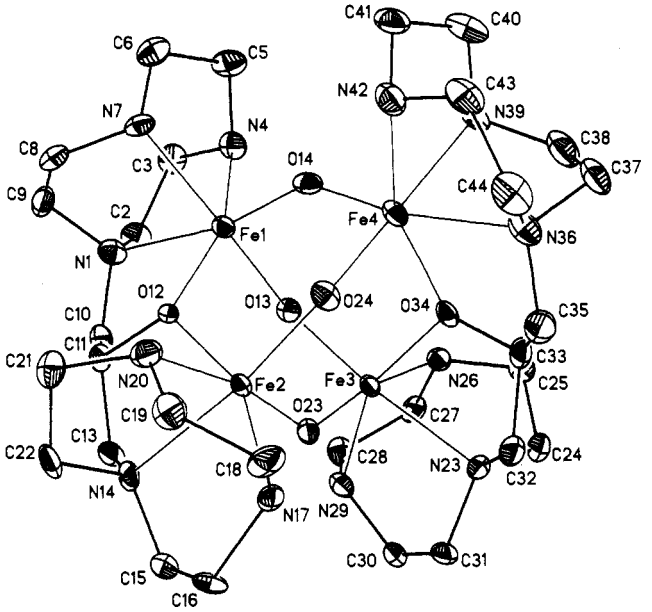

Figure 2. View of the cation of **4**, showing the atom-labeling scheme. Thermal ellipsoids are scaled to the 30% probability level. H atoms have been omitted for clarity. Relevant bond lengths and bond angles are summarized in Table III.

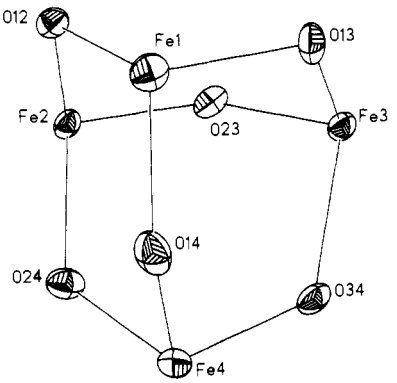

Figure 3. View of the adamantane-like geometry exhibited by the Fe_4O_6 core in **4**.

to be typical for this type of Fe_4O_6 cluster as it has also been observed by Que et al.[11h] and, to a lesser degree, in Wieghardt's tetranuclear iron complex.[11e] Apparently, as previously noted by Que,[11h] the need to maintain a reasonable Fe···Fe distance while accommodating the short Fe–O bonds results in the widening of the Fe–O–Fe bond angle.

Magnetic Susceptibility. Because of the symmetry in the adamantane-like core of complex **4**, there are three unique magnetic coupling pathways linking the four iron atoms (Figure 4). The pathways are distinguished from one another by the nature of the iron-to-iron bridging group (i.e. oxo, hydroxo, or alkoxo). As such, three different exchange coupling constants (J_{12}, J_{13}, J_{14}) are needed to describe these distinct pathways. Unfortunately, in the case where $J_{12} \neq J_{13} \neq J_{14}$, the individual coupling constants cannot be accurately determined without a full theoretical analysis.[26] We have, thus, used a model to provide a description for the magnetic behavior exhibited by **4**.

The model (see Figure 4) is based on two diiron(III) core units within the tetranuclear iron complex behaving as discrete magnetic entities. For our purposes, then, we have attributed all of the magnetic coupling observed in **4** to the two oxo-mediated pathways (J_{14} in Figure 4) and assumed the hydroxo- and alkoxo-mediated pathways to be zero. A literature survey of J values for μ-oxo, μ-hydroxo, and μ-alkoxo mono-bridged iron(III) dimers, in fact,

(26) Sinn, E. *Coord. Chem. Rev.* **1970**, *5*, 313–347.

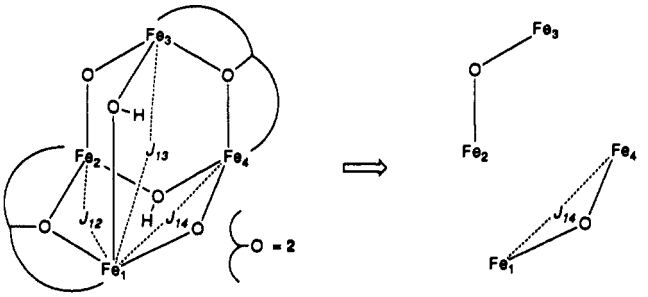

Figure 4. Three distinct exchange interactions in **4**, each governed by a unique coupling constant (J_{12}, J_{13}, J_{14}), modeled by figuratively removing the hydroxo and alkoxo bridges. This approximation produces two noninteracting, (μ-oxo)diiron(III) cores for which there is only one coupling pathway, J_{14}.

provides some insight into the severity of this assumption. Singly oxo-bridged iron(III) dimers have J values typically in the range of -80 to -105 cm^{-1}.[9] While there are fewer examples of hydroxo- and alkoxo-bridged diiron(III) complexes in the literature, there is, nonetheless, a particularly narrow range in which the J values are found (approximately -10 to -15 cm^{-1}).[9,11h] It is clear that while the hydroxo- and alkoxo-mediated pathways undoubtedly contribute to the overall antiferromagnetic coupling observed in **4** (i.e. J_{12}, $J_{13} \neq 0$), their contribution should be much smaller than that of the oxo-mediated pathway. Therefore, to provide a semiquantitative view of the antiferromagnetic behavior of **4**, we have emphasized in our model only the dominant magnetic exchange pathway, J_{14}.

In this case, the molar paramagnetic susceptibility data are fit to an expression, derived elsewhere,[27] which is based on the general isotropic exchange Hamiltonian, $H = -2JS_1S_2$, with J = magnetic exchange coupling constant and $S_1 = S_2 = {}^5/_2$:

$$\chi_m^{corr} = \frac{(1-p)C(2e^{2x} + 10e^{6x} + 28e^{12x} + 60e^{20x} + 110e^{30x})}{1 + 3e^{2x} + 5e^{6x} + 7e^{12x} + 9e^{20x} + 11e^{30x}} + \frac{4.375p}{T} + \text{TIP} \quad (1)$$

Here, $C = Ng^2\mu_B^2/kT$, $x = J/kT$, and p = mole percentage of paramagnetic impurity. The temperature-independent paramagnetic susceptibility term (TIP) was excluded because the ground state of high-spin iron(III) is much lower in energy than its first excited state.[28] The $4.375/T$ term accounts for the spin-only magnetism associated with a paramagnetic iron(III) ($S = {}^5/_2$) impurity of mole percentage "p". The value of g was fixed at 2.0 for all fits.

As shown in Figure 5, the susceptibility data are fit[29] extremely well by eq 1 ($R = 0.9994$) with $J = -93(2)$ cm^{-1} and $p = 4.27 \times 10^{-3}$. The value of J is typical for μ-oxo, mono-bridged diiron(III) complexes and demonstrates strong antiferromagnetic coupling. The magnetic properties of **4** are quite similar to those described for both Que's[11h] $(Fe(O)_2(OH)_2(OR)_2)^{4+}$ and Wieghardt's[11e] $(Fe_4(O)_2(OH)_4)^{4+}$complexes. To our knowledge, there are no reported J values for Que's tetranuclear complex; however, these workers do note a room-temperature magnetic moment of 1.74 μ_B/Fe which compares quite favorably with **4** (1.81 μ_B/Fe at 300 K; 0.26 μ_B/Fe at 40 K).[11h] Wieghardt et al. have reported for the $Fe_4(O)_2(OH)_4$ cluster both a magnetic moment of 1.94 μ_B/Fe at 299 K and J values for the oxo-mediated (-106 cm^{-1}) and hydroxo-mediated (-15 cm^{-1}) pathways.[11e]

Attempts to include an interdimer coupling interaction (i.e. between dimers) to approximate the hydroxo- and alkoxo-

(27) O'Connor, C. J. *Prog. Inorg. Chem.* **1982**, *29*, 203–283.
(28) Carlin, R. L. In *Magnetochemistry*; Springer-Verlag: Berlin, **1986**; p 64.
(29) Nonlinear parameter estimation and model development program: MINSQ. MicroMath Scientific Software, Salt Lake City, UT 84121.

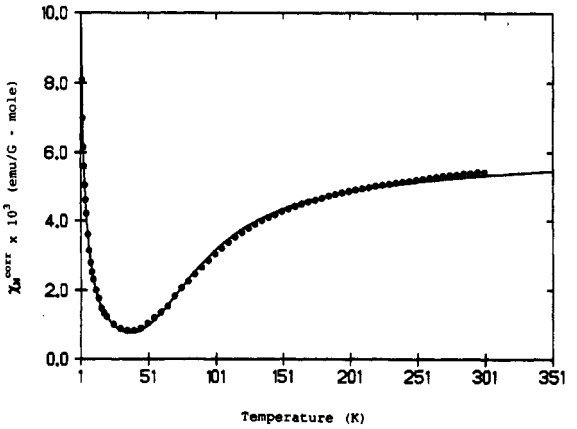

Figure 5. Plot of χ_M^{corr} (●) vs T for solid **4**. The line represents the best least-squares fit of eq 1 (see text) to the experimental susceptibility data.

mediated coupling in **4** did not improve the fit. With the assumption that the alkoxo- and hydroxo-mediated pathways are equivalent ($J_{12} = J_{13}$), the intramolecular coupling in **4** was treated by the molecular field approximation.[11e,11j,30] In this case, two exchange coupling constants are needed to describe the magnetic behavior: J, the intradimer coupling constant (J_{14} in Figure 4) and J', the interdimer coupling constant (J_{12} and J_{13} in Figure 4). The molar paramagnetic susceptibility data are then fit to the following expression:

$$\chi_m^{corr} = \frac{(1-p)2Ng^2\mu_\beta^2(A/B)}{k[T-2J'(A/B)]} + 4.375p/T + \text{TIP} \quad (2)$$

Here, $A = 2e^{2x} + 10e^{6x} + 28e^{12x} + 60e^{20x} + 110e^{30x}$, $B = 1 + 3e^{2x} + 5e^{6x} + 7e^{12x} + 9e^{20x} + 11e^{30x}$, $x = J/kT$, and p = mole percentage of paramagnetic impurity. As before, the contribution of the TIP term was assumed to be zero. With g fixed at 2.0, the least-squares fit of the data to eq 2 gave $J = -93$ cm^{-1}, $J' = 2$ cm^{-1} and $p = 4.27 \times 10^{-3}$ with no improvement over the fit using eq 1. Since J' is essentially zero the values for the exchange coupling constants in this equation are the same as that obtained from equation 1 ($J = -93$ cm^{-1}, $J' = 0$ (by definition)). Due to the excellent fit of the data to eq 1, the result for eq 2 is not wholly unexpected (i.e. eq 2 reduces to eq 1 when $J' = 0$). The small value of J' given by eq 2 probably does not reflect the actual contribution of J_{12} and J_{13} to the overall intramolecular coupling but, instead, is an indication that in the presence of both the dominant oxo-mediated coupling and the small paramagnetic impurity (assumed to be a monomeric Fe(III) complex), the smaller interdimer exchange coupling constant, J', cannot be quantitatively determined by this method. We conclude then that the magnetism exhibited by **4** is best approximated by assuming two noninteracting oxo-bridged diiron(III) cores which are each strongly antiferromagnetically coupled ($J = -93(2)$ cm^{-1}).

(30) O'Connor, C. J. *Prog. Inorg. Chem.* **1982**, *29*, 244–245.

Conclusion

We have synthesized the new ditopic receptor, **2**, and explored its ability to stabilize oxo-bridged, oligomeric Fe(III) complexes. Interestingly, in either the presence or absence of a carboxylate source, ligand **2** stabilizes the same tetranuclear iron(III) complex in which no carboxylate ligands are found. Furthermore, the same Fe(III) complex can be synthesized via an Fe(II) source followed by air oxidation. The resulting tetranuclear iron(III) complex, **4**, has been structurally characterized and found to contain an Fe_4O_6 core in an adamantane-like geometry with the iron atoms occupying the bridgehead positions. A model used to describe the strong antiferromagnetic coupling observed in **4** is based on two noninteracting oxo-bridged diiron(III) cores. In this model, the best fit of the data gives an exchange coupling constant, J, equal to $-93(2)$ cm^{-1}. We are currently interested in determining the nature of the Fe(II) precursor to complex **4** and in understanding the factors which govern the formation of tetranuclear vs dinuclear iron(III) species.

Acknowledgment. J.L.S. acknowledges the NIH (Grant No. GM 36348), the NSF (PYI Award 1986), and the Camille and Henry Dreyfus Foundation (New Faculty Award, 1984; Teacher-Scholar Award 1988) for partial funding for this work. J.T.M. thanks the Robert A. Welch Foundation (Grant No. F-1191).

Supplementary Material Available: For **4**, tables of anisotropic thermal parameters for the non-hydrogen atoms, positional and isotropic thermal parameters for the H atoms, bond lengths and angles, and torsion angles and a figure providing a view of a unit cell packing diagram (23 pages). Ordering information is given on any current masthead page.